第51卷第2期 中国科学技术大学学报 Vol. 51, No. 2
2021年2月 JOURNAL OF UNIVERSITY OF SCIENCE AND TECHNOLOGY OF CHINA Feb. 2021
Received: 2021-02-03; Revised: 2021-02-25 doi:10.52396/JUST-2021-0041

LncRNA GIMA promotes hepatocarcinoma cell survival via inhibiting ATF4 under metabolic stress

WANG Hong, LUO Jingjing, WANG Chenfeng, ZHANG Guang, MEI Yide*, YANG Yang*
School of Basic Medical Sciences, Division of Life Sciences and Medicine, University of Science and Technology of China, Hefei 230027, China
* Corresponding author. E-mail: meiyide@ustc.edu.cn; yangyang07@ustc.edu.cn

Abstract: Tumor cells are usually under nutrient-deficient microenvironment, a series of adaptive responses are adopted to maintain the cell survival and growth under the metabolic stress. However, the regulatory role of long non-coding RNA (lncRNA) in this process still remains elusive. To explore whether lncRNAs involve in regulating the hepatocarcinoma cell survival under the metabolic stress, GIMA (glucose-deprivation induced modulator of ATF4) was identified as an lncRNA induced by glucose deprivation via the transcriptome sequencing, and the upregulation of GIMA depends on the ATF4 activation under glucose deprivation. The Luciferase assay and the chromatin immunoprecipitation assay proved that GIMA is the transcriptional target gene of ATF4. Furthermore, GIMA promotes the hepatocarcinoma cell survival under glucose deprivation via specifically inhibiting ATF4. Taken together, these results suggest that GIMA may be a new potential target for the hepatocarcinoma treatment.

Keywords: lncRNA; GIMA; hepatocarcinoma; glucose deprivation; cell survival
CLC number: R735.7 **Document code**: A

1 Introduction

Tumor cells are surrounded by a completely different microenvironment than that of normal cells, so they must exhibit adaptive responses to hypoxia and nutrient-deficient conditions[1]. This phenomenon of alterations of tumor energy metabolism and nutrient uptake, called metabolic reprogramming, has been listed as one of important hallmarks of cancer[2]. For example, cancer cells preferentially utilize glucose to generate ATP and building blocks for biosynthetic processes regardless of oxygen availability, the so-called Warburg Effect[3]. Cancer cells also need to rewire metabolism to survive the nutrient stress such as glucose limitation [4]. Activating transcription factor 4 (ATF4) is a stress-induced transcription factor that is frequently up-regulated in cancers [5], a member of the ATF/CREB family, which plays a critical role in regulating genes involved in the integrated stress response (ISR), amino acid metabolism, redox homeostasis and ER stress responses[6,7]. These functions of ATF4 can be hijacked by cancer cells to sustain rapid proliferation and survive the harsh tumor microenvironment [8]. However, ATF4 may suppress tumor development under certain conditions and induces apoptosis[9-11]. Although the regulation of cancer metabolism by protein-coding genes has been studied extensively [12,13], the involvement of recently identified long non-coding RNA (lncRNA) in mediating tumor cell survival under stress remains largely unexplored.

Long non-coding RNA (lncRNA) is a type of RNA with a transcript longer than 200 nucleotides and with low protein-coding potential[14]. Next-generation sequencing technology allows researchers to annotate a previously unappreciated large number of lncRNAs, but there are a limited number of lncRNAs that have been functionally characterized so far[15]. To date, lncRNAs have been demonstrated by playing major roles in cell proliferation, autophagy, and apoptosis regulation process via various mechanisms including chromatin modification, epigenetic regulation, alternative splicing and translation control, etc.[16-18]. Compared with mRNAs, lncRNAs are less conserved among species and are often tissue-specific [19]. Increasing researches have shown that the abnormal lncRNA expression has significant correlation with human diseases, especially the development of malignant tumors [20-22]. Generally, lncRNA dysregulation affects the biological process such as the tumor proliferation, invasion and metastasis, leading to poor prognosis of cancer patients[23,24]. However, whether lncRNAs involve in the energy metabolism regulation still remains elusive.

Citation: WANG Hong, LUO Jingjing, WANG Chenfeng, et al. LncRNA GIMA promotes hepatocarcinoma cell survival via inhibiting ATF4 under metabolic stress. J. Univ. Sci. Tech. China, 2021, 51(2): 117-128.

In the past decades, hepatocarcinoma has become one of the deadliest malignant tumors worldwide, with the incidence and mortality rates increasing every year [25]. Among all cancers globally in 2018, hepatocarcinoma ranked sixth in incidence and fourth in mortality[26]. From 2000 to 2016 in the US mortality rate of hepatocarcinoma increased by 43%, making it the second deadliest cancer preceded only by pancreatic cancer. In China, the five-year survival rate of hepatocarcinoma patients was only as low as 12% [27]. In this study, using liver cancer as a model system to study cancer metabolism, we identified an lncRNA induced by glucose deprivation, named GIMA (glucose-deprivation induced modulator of ATF4), and glucose deprivation-induced GIMA was ATF4 dependent. Upon glucose deprivation, GIMA could prevent cell death via inhibiting the ATF4 protein expression.

2 Materials and methods

2.1 Cell culture

HEK293T cells (human embryonic kidney cells), PLC cells and HepG2 cells (human hepatocarcinoma cell line) were purchased from ATCC cell bank in USA, All cell lines were cultured at 37 °C, 5% CO_2 in DMEM + 10% fetal bovine serum (FBS) and were tested for mycoplasma contamination to ensure the reliability of the experimental data.

2.2 Nuclear and cytoplasmic separation experiment

When HepG2 cell density of the 6cm culture dish reached 80%−90%, digest and collect the cells into the EP tube and wash them with PBS. Cell pellets were gently resuspended in 100 μL Buffer I (1mmol · L^{-1} $MgCl_2$, 5 mmol · L^{-1} KCl, 25mmol · L^{-1} Tris-HCl (pH 7.4), 0.04% NP-40, 1×Protease Inhibitor Cocktail, 80U · mL^{-1} RNase inhibitor) and incubated for 5 min on ice. The centrifuge sample at 5000 g for 89 min at 4 °C, collect supernatant as the cytoplasm fraction.

The remaining cell pellets were washed 3 times with PBS, centrifuged at 5000 g at 4°C. Cell pellets (cell nucleus) were gently resuspended in 100 μL Buffer II (25 mmol · L^{-1} Tris-HCl (pH 7.4), 400 mmol · L^{-1}NaCl, 1 mmol · L^{-1} EDTA, 1mmol · L^{-1} EGTA, 0.5 mmol · L^{-1} DTT, 1×Protease Inhibitor Cocktail, 80 U · mL^{-1} RNase inhibitor) and incubated for 20 min on ice. Centrifuge sample at 12000 g for 10 min at 4 °C, collect supernatant as the nuclear fraction.

Detect the nuclear and cytoplasmic distribution of protein and RNA by western blot and qPCR, respectively.

2.3 Real-time fluorescent quantitative PCR (RT-qPCR)

Total RNA was extracted with TRIzol (Invitrogen) reagent, and 1μg RNA fragment was synthesized into cDNA using PrimeScript TM RT kit (Takara, DRR037A). Use SYBR premix EX Taq (TaKaRa) for real-time PCR and StepOnePlus real-time PCR system for analysis (Thermo Fisher Scientific). The PCR results, recorded as threshold cycle (Ct) numbers, were normalized against an internal control (actin). The expression data was analyzed using the 2-ΔΔCT method. The primer sequences are shown in Table 1.

2.4 RNA-FISH (RNA fluorescence in situ hybridization)

The subcellular localization of GIMA in hepatocarcinoma cells was determined using an Alexa Fluor 488 labeled antisense probe (nucleic acid labeling kit; Invitrogen). RNA-FISH was performed using the nucleic acid labeling kit according to the manufacturer's instructions. HepG2 cells were fixed in 4% paraformaldehyde for 10 min on ice and then permeabilized using 0.5% Triton X-100 in the CSK buffer for 5 min at room temperature. After dehydration with ethanol to 70% and then 100%, cells were probed overnight the biotinylated oligo (dT) at 37 °C in the presence of 15% formamide. After several washes in the SSC buffer (4×, 2×, and 1×) cells were stained for 3 h (at 37 °C) with Alexa 488−conjugated streptavidin in a buffer with 4× SSC buffer and 1% of RNase-free bovine serum albumin (Invitrogen/Life Technologies, Carlsbad, CA). Images were digitally acquired on a microscope.

2.5 5′RACE and 3′RACE

The 5′RACE measurements were conducted according to the manufacturer's instructions [SMARTer RACE 5′/3′ kit (Clontech)]. Briefly, total RNA was extracted from HepG2 cells with TRIzol reagent (Invitrogen Life Technologies). PCR reactions were performed using the universal primers provided in the 5′RACE kit. The PCR product was cloned and sequenced. The primer sequences of P1 and P2 are shown in Table 1.

2.6 Lentivirus packaging

To generate lentiviruses expressing the indicated shRNAs, HEK293T cells were transfected with shRNAs (cloned in PLKO.1), pREV, pGag/Pol/PRE, and pVSVG with a ratio of 2∶2∶2∶1 using Lipofectamine 2000 (Invitrogen) Transfection Reagent. To generate lentiviruses expressing pSin empty vector (control) or the indicated genes, HEK293T cells were transfected with pSin-based construct, pMD2.G, and psPAX2 with a ratio of 2∶1∶2 using Lipofectamine 2000 (Invitrogen) Transfection Reagent. For generation of the control virus, PLKO.1 or pSin empty vector was used. 4−6 h after transfection, the culture medium was replaced with fresh medium. 48 h later, the medium containing lentiviral particles was collected by filtration with 0.45 μm PVDF membrane (Millipore). The shRNA sequences used in this study are shown in Table 1.

2.7 Chromatin immunoprecipitation assay (ChIP)

According to the instructions of the chromatin immunoprecipitation kit (Beyotime), HepG2 cells were cross-linked with 1% formaldehyde for 10 min. Then cells were lysed and ultrasonically disrupted. The ATF4 antibody and normal rabbit immunoglobulin G (IgG) were used for the chromatin immunoprecipitation experiment. The bound DNA fragments were detected by PCR using the specific primers.

2.8 Luciferase reporter assay

The JASPAR database was used to predict the potential binding sequence of ATF4 on the GIMA promoter to construct a luciferase reporter gene system. Control vector (ctrl), Flag-ATF4 was co-transfected with renilla luciferase plasmid, pGL3-basic vector/pGL3-basic vector containing GIMA wild-type or mutant binding sites respectively. We applied Lipofectamine 2000 (Invitrogen) Transfection Reagent for the experiment. 24 h later, the activity of the reporter system was measured by the luciferase assay kit (Promega), and the renilla luciferase activity was used as an internal reference for plotting (mean ±SD).

2.9 ROS Level measurement

Refer to the instructions of the Reactive Oxygen Species Assay Kit (Beyotime), use HepG2 and PLC cells as experimental materials, and dilute DCFH-DA with serum-free culture medium at 1∶1000 to make the final concentration 10μmol · L^{-1}.

After cells being collected, suspended in the diluted DCFH-DA, the cell concentration was $1\times10^6-2\times10^7$ cells · mL^{-1}. Incubate for 20 min in a 37 °C cell incubator. Invert and mix every 3-5 min to make the probe and the cells fully contact. Wash the cells three times with serum-free cell culture medium to fully remove the DCFH-DA that has not entered the cells. Guava EasyCyte HT Flow Cytometer (Millipore) was used to detect the ROS level, and the 488nm excitation wave length was used to detect the intensity of cell fluorescence.

2.10 Cell viability assay

The cell viability was measured by propidium iodide (PI) staining. The cells were stained with PI (final concentration: 50 μg · mL^{-1}) and hoechst (final concentration: 1 μg · mL^{-1}) for 20 min and then observed by the inverted fluorescence microscope (Olympus) and photographed by software, finally counted manually.

2.11 Cell proliferation assay

PLC and HepG2 cells were infected with lentiviruses expressing control shRNA, GIMA shRNA#1, GIMA shRNA#2 or control, GIMA, respectively. 48 h later, cells were seeded to 24-well plate. Number of cells was measured by the Countstar BioTech Automated Cell Counter (Shanghai Ruiyu) every day for up to 4th day.

2.12 Quantification and statistical analysis

SPSS 21.0 statistical software was used to analyze the data, and the analysis of the differences between sample data was calculated by the t-test statistical method. A p value <0.05 indicates that the difference is statistically significant. *, ** and *** represent p-values less than 0.05, 0.01 and 0.001, respectively. Ns, means no significance.

3 Results

3.1 Metabolic stress induces lncRNA GIMA expression

To identify the metabolic stress-induced lncRNAs, we conducted an RNA sequencing experiment in hepatocellular carcinoma (HCC) HepG2 cells cultured in normal or glucose-free medium. Eight identified lncRNAs that are triggered by glucose starvation were validated by quantitative PCR. These lncRNAs were selected based on on fold change (≥2) and p value (<0.05) under glucose deprivation (Table 2). Among the lncRNAs examined, lnc-GPR89B-11∶2 was the most up-regulated (Figure 1(a)). We next further confirmed the up-regulation of lnc-GPR89B-11∶2 upon glucose deprivation. Indeed, the expression level of lnc-GPR89B-11∶2 was elevated during the time course in response to glucose starvation both in PLC and HepG2 cells (Figure 1(b, c)). Thus, we focused on lnc-GPR89B-11∶2 and, for simplicity, refer this lncRNA as GIMA (glucose-deprivation induced modulator of ATF4) given that it is able to specifically regulate the protein level of ATF4. GIMA was predominantly localized in the nucleus (Figure 1(d, e)). GIMA is located on chromosome 1 of the human genome. By performing rapid-amplification of complementary DNA (cDNA) ends (RACE) experiments, GIMA was revealed as an RNA transcript with a molecular size of 4432nt (Figure 1(f, g)), which is 17 nucleotides more at the 5′end than the reference sequence of lnc-GPR89B-11∶2 on LNCipedia. The above results indicate that LncRNA GIMA is induced by glucose deprivation in hepatocarcinoma cells.

3.2 Induction of GIMA is dependent on ATF4 in response to glucose deprivation

To interrogate how GIMA is induced upon glucose deprivation, we used the JASPAR database to inspect the upstream region of the GIMA gene. Two putative ATF4 binding sites (P1 and P2) were identified. As reported previously [28], the expression level of ATF4 increases significantly under the metabolic stress such as glucose starvation, and then ATF4 transcriptionally activates the downstream target genes involved in the adaptive survival response. We therefore asked whether ATF4 was responsible for glucose deprived induction of GIMA. Glucose starvation consistently induced GIMA in HepG2 cells. However, this increased GIMA

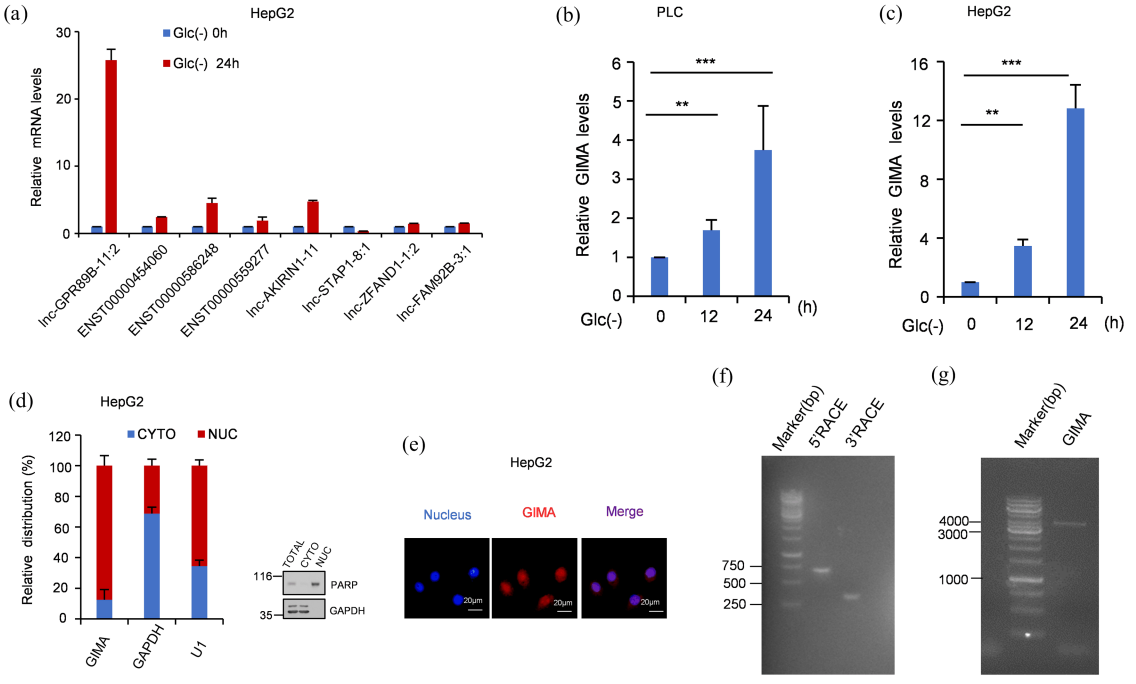

Figure 1. LncRNA GIMA is induced by glucose deprivation. (a) RT- qPCR showing expression level of 8 identified lncRNAs that are triggered by glucose starvation in HepG2 cells cultured in glucose-free medium for 24 h. Data shown are mean ±SD ($n=3$). (b,c) RT- qPCR showing expression level of GIMA in HepG2 and PLC cells cultured in glucose-free medium during the time course(0h,12h, 24h). Data shown are mean ±SD ($n=3$). **, $p<0.01$; ***, $p<0.001$. (d) Subcellular fractionation followed by RT-qPCR for GIMA in HepG2 cells. Data shown are mean ±SD ($n=3$). (e) RNA-FISH (RNA fluorescence in situ hybridization) for GIMA in HepG2 cells. Nuclei are counter-stained with 4′,6-diamidino-2- phenylindole (DAPI). (f) Shown are products obtained from 5′-RACE (rapid amplification of cDNA ends) and 3′-RACE experiments. (g) Shown is the full length of GIMA.

expression was abolished when ATF4 was knocked down (Figure 2(a)), indicating that ATF4 is indispensable for the induction of GIMA under glucose deprivation. Next, we explored whether ATF4 regulates GIMA expression at the transcriptional level. The knockdown of ATF4 decreased, whereas overexpression of ATF4 increased the expression level of GIMA in both PLC and HepG2 cells(Figure 2(b-e)). The chromatin immunoprecipitation assay (ChIP) demonstrated that ATF4 co-precipitated with the chromatin fragment comprising P1 and P2, respectively, upon glucose deprivation (Figure 2(f)). To examine whether P1 or P2 site confers ATF4-dependent transcriptional activity, luciferase reporter assay was carried out. The ectopic expression of ATF4 markedly increased the transcriptional activity of luciferase reporter containing wild-type P1 and P2 sites, respectively, whereas the mutation of P1 and P2 completely diminished the increased activity (Figure 2(g)). Collectively, glucose deprivation-induced GIMA is ATF4-dependent.

3.3 GIMA protects hepatocarcinoma cells from glucose deprivation-induced death

We next investigated the potential function of GIMA in mediating metabolic stress response. To avoid off-target effects, two different GIMA targeting shRNAs (sh-GIMA#1 and sh-GIMA#2) were used. Both of these two shRNAs were able to efficiently decrease GIMA expression in both PLC and HepG2 cells (Figure 3(a, b)). GIMA knockdown significantly sensitized both of HepG2 and PLC cells to glucose deprivation-induced death (Figure 3(e,f)), which could be rescued by ectopic expression of shRNA-resistant form of GIMA (Figure 3(g-j)). In addition, neither the depletion nor overexpression of GIMA was shown to affect the proliferation of both HepG2 and PLC cells (Figure 3(a-d, k-n)), precluding the effect of proliferation rates on the glucose deprivation-induced cell death. These results demonstrate that GIMA plays a previously unreported protective function in the hepatocarcinoma cell survival under glucose deprivation.

The glucose deprivation-induced cell death was also restored in GIMA knockdown cells by replenishing the cells with N-acetyl-L-cysteine (NAC), a well-known antioxidant which effectively scavenges ROS (Figure 4(a,b)). We therefore proposed that GIMA may regulate cellular ROS levels to prevent cell death from glucose deprivation. In support of this, the knockdown of GIMA in PLC and HepG2 cells increased ROS levels under glucose deprivation, however, which was rescued by the overexpressing shRNA-resistant form

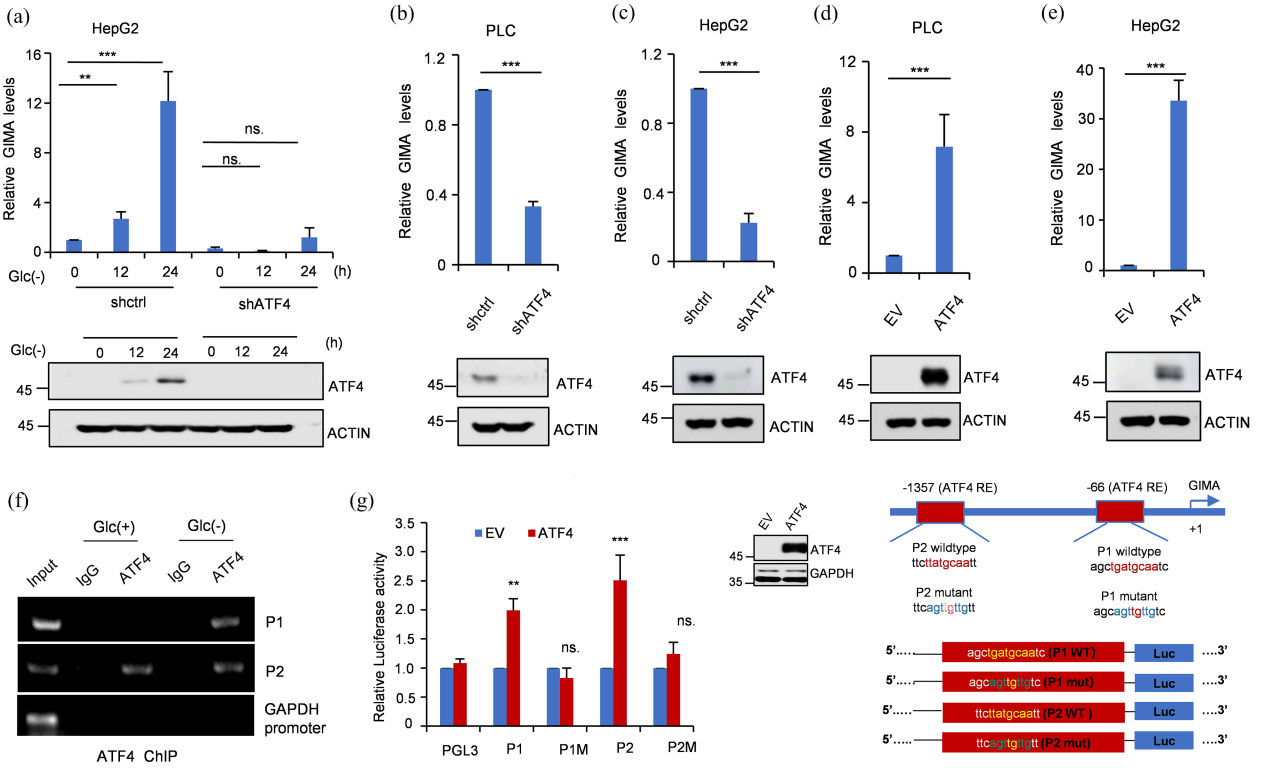

Figure 2. Glucose deprivation-induced GIMA is ATF4-dependent. (a) RT-qPCR detection of expression of GIMA in HepG2 cells treated with glucose-free medium during the time course (0h, 12h, 24h). Expression in each condition is shown relative to control (shctrl, shATF4). Data shown are mean ±SD ($n=3$). **, $p<0.01$; ***, $p<0.001$; ns., no significance. (b,c) RT-qPCR detection of expression of GIMA in PLC and HepG2 cells upon each condition (shctrl, shATF4). Data shown are mean ±SD ($n=3$). ***, $p<0.001$. (d,e) RT-qPCR detection of expression of GIMA in PLC and HepG2 cells upon each condition (EV, ATF4). Data shown are mean ±SD ($n=3$). ***, $p<0.001$. (f) Lysates from HepG2 cells were subjected to ChIP assay using anti-ATF4 antibody or an isotype-matched control immunoglobulin G (IgG). Three independent experiments were done with the similar results. Results from one experiment are shown. (g) Shown are the pGL3-based wild-type and mutant reporter constructs used for luciferase (Luc) assay. HEK293T cells were co-transfected with control vector (ctrl), or Flag-ATF4, together with the reporter constructs in the indicated combination. Twenty-four hours after transfection, reporter activity was measured and plotted after normalizing with respect to renilla luciferase activity. Data shown are mean ±SD ($n=3$). **, $p<0.01$; ***, $p<0.001$; ns., no significance. HEK293T cells were transfected with control vector (ctrl) or Flag-ATF4, and the cells were collected 24 hours later to detect the overexpression of ATF4 (using endogenous ATF4 antibody).

of GIMA (Figure 4(c–f)). We noticed that under normal conditions, the knockdown of GIMA had no effect on cellular ROS levels (Figure 4(g–j)), implying that GIMA may exert its function in response to the metabolic stress. Taken together, our data reveal that GIMA may prevent the glucose deprivation-induced death in hepatocarcinoma cells via reducing cellular ROS levels.

3.4 GIMA promotes hepatocarcinoma cells survival via inhibiting ATF4 expression under glucose deprivation

To explore the molecular mechanism whereby GIMA protects hepatocacinoma cells from glucose deprivation-induced death, we examined whether GIMA could modulate protein levels of glucose metabolism-related genes such as PHGDH, G6PD, PSAT1, PSPH and LDHA. The results showed that the protein levels of these glucose metabolism-related genes were not affected by GIMA depletion under both normal and glucose deprived conditions (Figure 5(a, b)). However, intriguingly, the knockdown of GIMA dramatically increased the protein level of ATF4 under glucose deprivation (Figure 5(c)). Similar results were also obtained in HepG2 cells (Figure 5(d)), indicating that GIMA may specifically inhibit the ATF4 expression. Given the inhibitory effect of GIMA on the ATF4 protein expression, we sought to evaluate whether GIMA facilitates cell survival under glucose deprivation via ATF4. We knocked down GIMA, ATF4 or both of GIMA and ATF4 in HepG2 and PLC cells. GIMA knockdown consistently decreased cell viability under glucose deprivation, which could be restored by the simultaneous knockdown of ATF4 (Figure 5(e, f)). Collectively, these data suggest that GIMA may promote hepatocarcinoma cells survival under glucose deprivation via inhibiting the ATF4 expression.

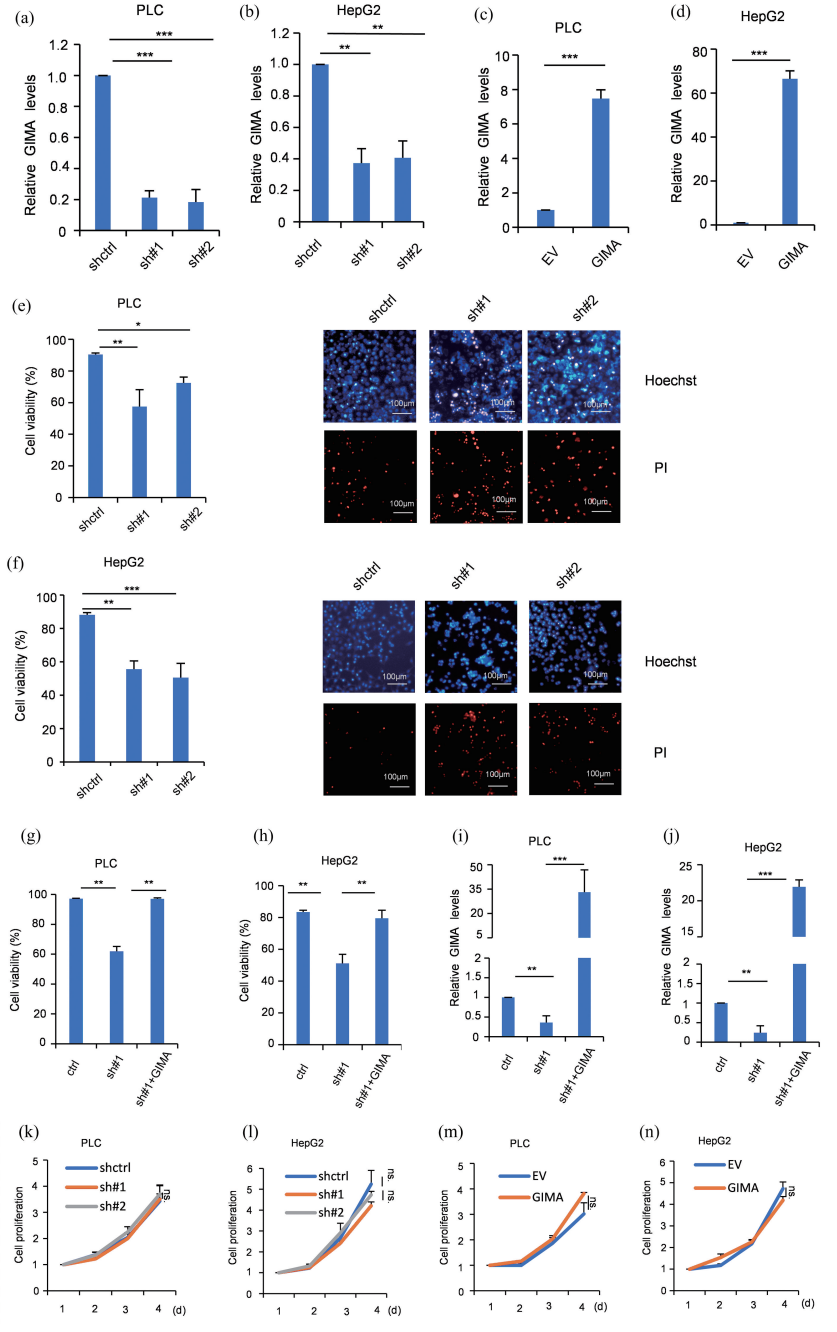

Figure 3. GIMA protects hepatocarcinoma cells from glucose deprivation-induced death. (a,b) The knockdown efficiency of GIMA was verified by real-time RT-qPCR analysis in PLC and HepG2 cells. Data shown are mean ±SD ($n=3$). **, $p<0.01$; ***, $p<0.001$. (c,d) The successful overexpression of GIMA was determined by real-time RT-qPCR analysis. Data shown are mean ±SD ($n=3$). ***, $p<0.001$. (e,f) PLC and HepG2 cells were infected with lentiviruses expressing control shRNA, GIMA shRNA#1, GIMA shRNA#2. Forty-eight hours later, cells were cultured under glucose deprivation. Seven-two hours later, cells were assayed for their viability. The shown images are representative of three independent experiments. Data shown are mean ±SD ($n=3$). *, $p<0.05$; **, $p<0.01$ ***, $p<0.001$. (g,h) PLC and HepG2 cells were infected with lentiviruses expressing control shRNA, GIMA shRNA#1, shRNA-resistant GIMA. Forty-eight hours later, cells were cultured under glucose deprivation. Seven-two hours later, cells were assayed for their viability. The shown images are representative of three independent experiments. Data shown are mean ±SD ($n=3$). **, $p<0.01$. (i,j) PLC and HepG2 cells were infected with lentiviruses expressing control shRNA, GIMA shRNA#1, shRNA-resistant GIMA. Forty-eight hours later, the knockdown efficiency of GIMA was verified by real-time RT-qPCR analysis. **, $p<0.01$ ***, $p<0.001$. (k,l) PLC and HepG2 cells were infected with lentiviruses expressing control shRNA, GIMA shRNA#1, GIMA shRNA#2. Forty-eight hours later, the cell growth curves were measured. Data shown are mean ±SD ($n=3$). ns., no significance. (m,n) PLC and HepG2 cells were infected with lentiviruses expressing control, GIMA. Forty-eight hours later, the cell growth curves were measured. Data shown are mean ±SD ($n=3$). ns., no significance.

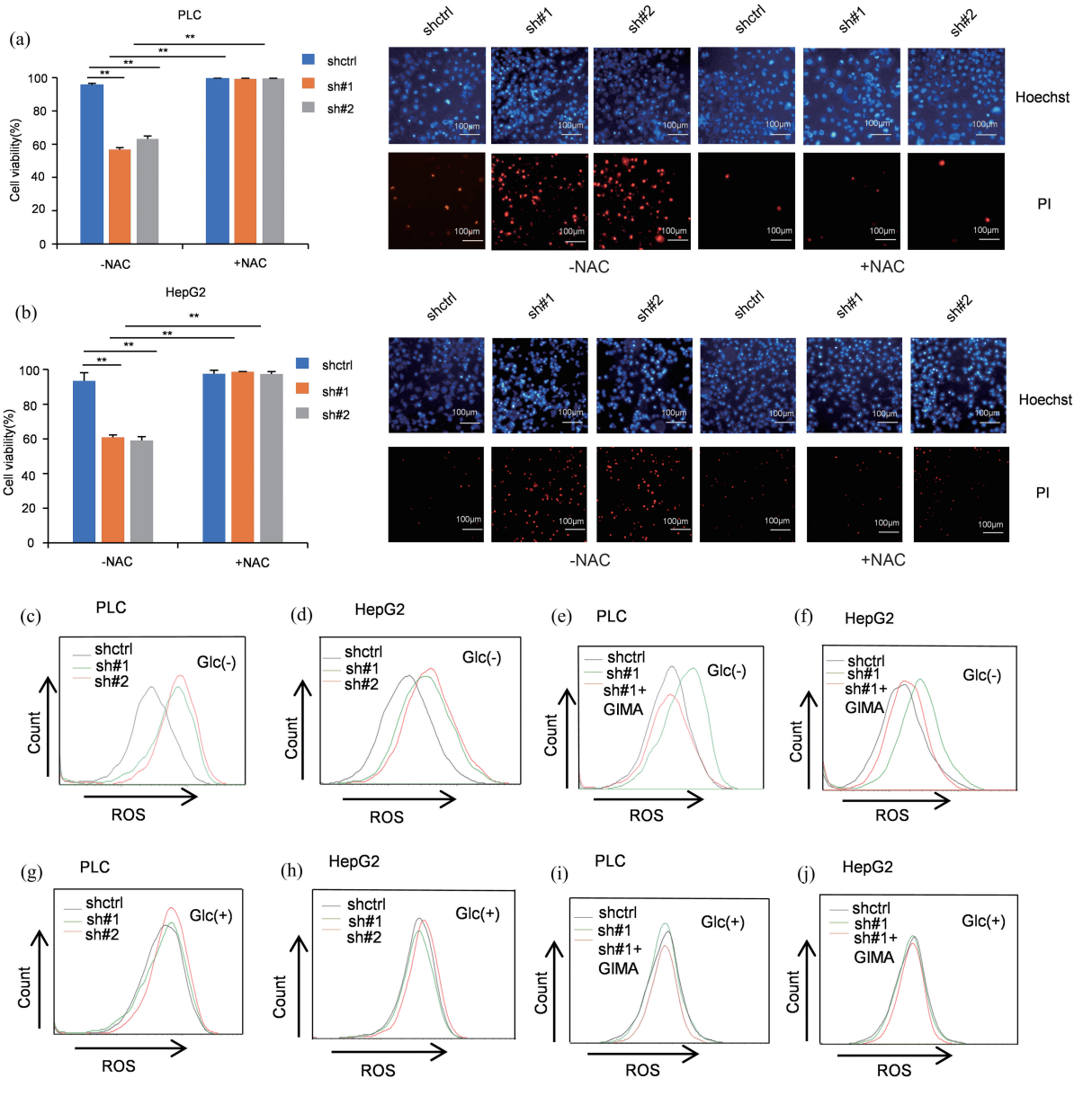

Figure 4. GIMA prevents glucose deprivation-induced death in hepatocarcinoma cells via reducing cellular ROS levels. (a,b) PLC and HepG2 cells were infected with lentiviruses expressing control shRNA, GIMA shRNA#1, GIMA shRNA#2 with or without NAC treatment. Forty-eight hours later, cells were cultured under glucose deprivation. Seven-two hours later, cells were assayed for their viability. Data shown are mean ±SD (n=3). **, p<0.01. (c,d) PLC and HepG2 cells were infected with lentiviruses expressing control shRNA, GIMA shRNA#1, GIMA shRNA#2. Forty-eight hours later, cells were cultured under glucose deprivation. Seven-two hours later, ROS levels were detected by flow cytometry. (e,f) PLC and HepG2 cells were infected with lentiviruses expressing control shRNA, GIMA shRNA#1, shRNA-resistant GIMA. Forty-eight hours later, cells were cultured under glucose deprivation. Seven-two hours later, ROS levels were detected by flow cytometry. (g,h) PLC and HepG2 cells were infected with lentiviruses expressing control shRNA, GIMA shRNA#1, GIMA shRNA#2. Seven-two hours later, ROS levels were detected by flow cytometry. (i,j) PLC and HepG2 cells were infected with lentiviruses expressing control shRNA, GIMA shRNA#1, shRNA-resistant GIMA. Seven-two hours later, ROS levels were detected by flow cytometry.

4 Discussion

Cancer cells are known to develop strategies to sustain growth and survive nutrient-limited microenvironment, one of which is to maintain high levels of glycolysis under metabolic stress[29]. In response to glucose starvation, nuclear receptor Nur77 has been reported to prevent glucose deprivation-induced cell death in melanoma by protecting fatty acid oxidation[30]. The GCN2-ATF4 pathway is also critical for the cancer cell survival and growth in response to nutrient deprivation[31]. Via transcriptional regulation of downstream target

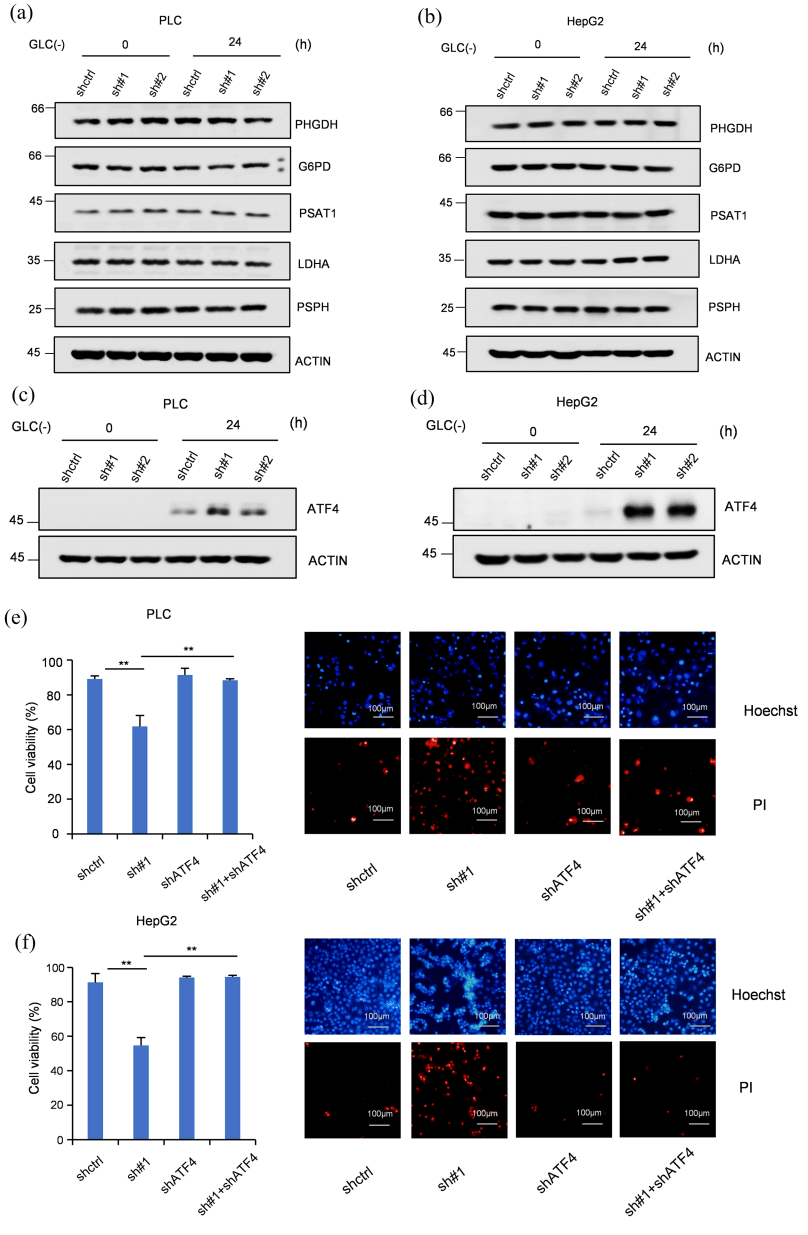

Figure 5. GIMA promotes hepatocarcinoma cells survival under glucose deprivation by inhibiting ATF4 expression. (a,b) Immunoblot for PHGDH, G6PD, PSAT1, PSPH and LDHA in GIMA silenced PLC and HepG2 cells under Glc (+)/Glc (−). (c,d) Immunoblot for ATF4 in GIMA silenced PLC and HepG2 cells under Glc (+)/Glc (−). (e,f) PLC and HepG2 cells were infected with lentiviruses expressing control shRNA, GIMA shRNA#1, ATF4 shRNA or both GIMA shRNA#1 and ATF4 shRNA. Forty-eight hours later, cells were cultured under glucose deprivation. Seven-two hours later, cells were assayed for their viability. The shown images are representative of three independent experiments. Data shown are mean ±SD ($n=3$). **, $p<0.01$.

genes, ATF4 engages in regulations of amino acid uptake and biosynthesis, autophagy, redox balance and angiogenesis process, promoting metabolic homeostasis and cancer cell survival[32]. However, induction of ATF4 also induces apoptosis under certain conditions. Jaeseok Han et al. found that the increased protein synthesis triggered by ATF4 generated ROS, which is a necessary signal to induce apoptosis under ER stress[33].

In this study, we screened and identified a glucose deprivation-induced LncRNA-GIMA. Recently several lncRNAs involved in regulating tumor energy metabolism have been reported. For instance, lncRNA FILNC1 and NBR2 are also induced by glucose deprivation. FILNC1 is shown to inhibit the glycolysis pathway via c-Myc, thereby suppressing the development of kidney cancer. In addition, the expression level of FILNC1 is down-regulated in renal cell carcinoma, which is positively correlated with the poor clinical prognosis of renal cell carcinoma [34]. Liu Xiaowen et al. [35] found that NBR2 is induced through

LKB1-AMPK pathway under the metabolic stress, which in turn interacts with AMPK and promotes AMPK kinase activity, thereby forming positive feedbacks to enhance the AMPK pathway under the metabolic stress, ultimately promoting the cellular uptake of nutrients such as amino acids and glucose. We here show that glucose deprivation-induced lncRNA GIMA is able to promote hepatocarcinoma cells survival via specifically inhibiting the ATF4 expression. Our study therefore reveals a previously unappreciated function of lncRNA in protecting cells from glucose deprivation-induced death.

By performing the chromatin immunoprecipitation (ChIP) and luciferase reporter assay, we show that GIMA is a direct target of ATF4. And glucose deprivation-induced GIMA is dependent on ATF4. Further, the knockdown of GIMA markedly induced cell death by increasing levels of cellular ROS upon glucose-free conditions. Mechanically, GIMA depletion dramatically increased the expression of ATF4, so we demonstrated a negative feedback regulation between ATF4 and GIMA. ATF4 transcriptionally activates GIMA; in turn GIMA can specifically inhibit ATF4 protein expression, thereby facilitating cell survival under glucose deprivation. In summary, our findings suggest that GIMA may be a new potential target for the treatment of hepatocarcinoma, providing new strategies for hepatocarcinoma prevention and treatment.

Table 1. Oligonucleotides used in this study.

Primers used in qRT-PCR assays	
β-Actin	Fw: 5′GACCTGACTGACTACCTCATGAAGAT3′
	Rev: 5′GTCACACTTCATGATGGAGTTGAAGG3′
lnc-GPR89B-11∶2	Fw: 5′GGATCGGCCCTTTCTTCAAATA3′
	Rev: 5′GTCTTTCCAGTTGGTGGTACTG3′
ENST00000454060	Fw: 5′GAGGCATATCTACTGGGAACAC3′
	Rev: 5′GGTGCCTTGCATGTTGATATTT3′
ENST00000586248	Fw: 5′CAGTGAAAGAAGGTCCCAGTAG3′
	Rev: 5′CCAGTAGCAGGATGTGATGATT3′
ENST00000559277	Fw: 5′CACAACCCTCCACCTTCTAAA3′
	Rev: 5′GGAAGTAGGGAAGTCTGTTCAC3′
lnc-AKIRIN1-11	Fw: 5′CCAAGGACGCTGGAACTATT3′
	Rev: 5′CCTCTTATCCAGGCCATAAGC3′
lnc-STAP1-8∶1	Fw: 5′TACAGGGTCACCTCTGAAGCA3′
	Rev: 5′TGAATCTCATGAGGCGCTGAA3′
lnc-ZFAND1-1∶2	Fw: 5′TCTGCATTTGGTAGTCCGGG3′
	Rev: 5′AACCACCAACACACTCCAGA3′
lnc-FAM92B-3∶1	Fw: 5′TAATGGACACGCAAGGCTGT3′
	Rev: 5′AGCCTGGCTGAGAACTTTTGT3′
RACE primers	
GIMA 5’-GSP1	5′CCCAGGCCCGGAAGGACAAGTAGGGGA3′
GIMA 5’-GSP2	5′CCGCAAGGGATCCCTTTCTGACGGG3′
GIMA 3’-GSP1	5′GAGTGAAGACTTGAAGGGGTGGTGG3′
GIMA 3’-GSP2	5′CCCTAGTGCCTGGTGCAGGGTAAGTAC3′

(*To be continued on the next page*)

(*Continued*)

Primers used in ChIP assays	
P1	Fw: 5′AAGCGCAAGAAACATGAAT3′
	Rev: 5′CTTTTGGGAATTTATTTTTTCT3′
P2	Fw: 5′TCTTCTCAACTTTTCTAT3′
	Rev: 5′CAGTGGCTTTCCCTGTCTC3′
GAPDH promoter	Fw: 5′TACTAGCGGTTTTACGGGCG3′
	Rev: 5′TCGAACAGGAGGAGCAGAGAGCGA3′
Oligonucleotide sequence of shRNAs	
sh-GIMA#1	5′GGACAGGAAATCACGAATT3′
sh-GIMA#2	5′GGAGATGGCGCTTAACATT3′
shATF4	5′GCCTAGGTCTCTTAGATGATT3′
Probe sequence used for RNA ISH	
CCUCUUGGTGCCCUGUTUCTTGGTCUUUCUTTUTGCTGGGTGTGTCTGTGUGCUTGGTTTTGGUTGUGUTTUUCUTTTGUUTC UGTUCUCTGUUTUUUGCTTUTTTCTTTCCCCUGTUGUTGUTCCTCUTCCUUTCUCTTUUUGGCCTGUUTUGUUCCUUUUGTCT GUCCTGCCCUTGUGTUUGUGUGUGCTCCTTCTGCCTGUTTGCTTCUGCTGUGUTUTCUGCCTTTTCCTGCCTTTGGUUTTGUUC	

Table 2. Screened lncRNA information.

Sequence Name	*p*-value	Absolute Fold change (Glc+ vs Glc-)	Regulation (Glc+ vs Glc-)	Chromosome	Type
lnc-GPR89B-11：2	7.81E−06	20.62906668	up	chr1	noncoding
ENST00000454060	0.011771	6.161658024	up	chr13	noncoding
ENST00000586248	0.002734	5.660763832	up	chr19	noncoding
ENST00000559277	0.000602	5.368126438	up	chr15	noncoding
lnc-AKIRIN1-11	3.3E−05	4.621190732	up	chr1	noncoding
lnc-STAP1-8：1	0.011328	4.025095531	up	chr4	noncoding
lnc-ZFAND1-1：2	0.007928	3.57252091	up	chr8	noncoding
lnc-FAM92B-3：1	0.038042	3.394886931	up	chr16	noncoding

Acknowledgments

This work was supported by the Fundamental Research Funds for Central Universities (YD9100002012 and WK9100000024) and Collaborative Innovation Programs of Hefei Science Center, CAS (2019HSC-CIP010).

Conflict of interest

The authors declare no conflict of interest.

Author information

WANG Hong is currently a Master student under the supervision of Prof. Mei Yide at University of Science and Technology of China. Her research interest mainly focuses on long non-coding RNAs.

MEI Yide (corresponding author) received his PhD degree from University of Science and Technology of China. He is currently a professor at University of Science and Technology of China. His research interests include signal pathways mediated by oncoproteins and tumor suppressor proteins and their roles in tumor formation, especially the molecular mechanisms of non-coding RNAs involved in tumor formation.

YANG Yang (corresponding author) received his PhD degree from University of Science and Technology of China. He is currently a postdoctoral researcher at the Division of Life Sciences and Medicine of University of Science and Technology of China.

References

[1] Tameemi W A, Dale T P, Jumaily R M K A, et al. Hypoxia-modified cancer cell metabolism. Front. Cell Dev. Biol., 2019, 7:4.

[2] Pavlova N N, Thompson C B. The emerging hallmarks of cancer metabolism. Cell Metab., 2016, 23(1):27-47.
[3] Liberti M V, Locasale J W. The Warburg Effect: How does it benefit cancer cells?. Trends Biochem. Sci., 2016, 41(3):211-218.
[4] Birsoy K, Possemato R, Lorbeer F K, et al. Metabolic determinants of cancer cell sensitivity to glucose limitation and biguanides. Nature, 2014, 508(7494):108-112.
[5] Zeng P, Sun S N, Li R, et al. HER2 upregulates ATF4 to promote cell migration via activation of ZEB1 and downregulation of E-cadherin. Int. J. Mol. Sci., 2019, 20(9):2223
[6] Zong Y, Feng S J, Cheng J W, et al. Up-regulated ATF4 expression increases cell sensitivity to apoptosis in response to radiation. Cell. Physiol. Biochem., 2017, 41(2):784-794.
[7] Gwinn D M, Lee A G, Campo M B M D, et al. Oncogenic KRAS regulates amino acid homeostasis and asparagine biosynthesis via ATF4 and alters sensitivity to L-asparaginase. Cancer Cell, 2018, 33(1):91-107. e6.
[8] Rozpedek W, Pytel D, Mucha B, et al. The role of the PERK/eIF2α/ATF4/CHOP signaling pathway in tumor progression during endoplasmic reticulum stress. Curr. Mol. Med., 2016, 16(6):533-544.
[9] Tang Q, Ren L W, Liu J Y, et al. Withaferin a triggers G2/M arrest and intrinsic apoptosis in glioblastoma cells via ATF4-ATF3-CHOP axis. Cell Prolif., 2020, 53(1): e12706.
[10] Liu H C, Chao X, Liu J W, et al. Aspirin exerts anti-tumor effect through inhibiting Blimp1 and activating ATF4/CHOP pathway in multiple myeloma. Biomed. Pharmacother., 2020, 125:110005.
[11] Iurlaro R, Püschel F, Annicchiarico C L L, et al. Glucose deprivation induces ATF4-mediated apoptosis through TRAIL death receptors. Mol. Cell. Biol., 2017, 37(10): e00479-16.
[12] Dayton T L, Jacks T, Heiden M G V. PKM2, cancer metabolism, and the road ahead. EMBO Rep., 2016, 17(12):1721-1730.
[13] Taguchi K, Yamamoto M. The KEAP1-NRF2 system in cancer. Front Oncol., 2017, 7:85.
[14] Qian X Y, Zhao J Y, Yeung P Y, et al. Revealing lncRNA structures and interactions by sequencing-based approaches. Trends Biochem. Sci., 2019, 44(1):33-52.
[15] Jathar S, Kumar V, Srivastava J, et al. Technological developments in lncRNA biology. Adv. Exp. Med. Biol., 2017, 1008:283-323.
[16] Liu Y, Yang Y L, Li L, et al. LncRNA SNHG1 enhances cell proliferation, migration, and invasion in cervical cancer. Biochem. Cell Biol., 2018, 96(1):38-43.
[17] Liu C Y, Zhang Y H, Li R B, et al. LncRNA CAIF inhibits autophagy and attenuates myocardial infarction by blocking p53-mediated myocardin transcription. Nat. Commun., 2018, 9(1):29.
[18] Chen L, Yang W J, Guo Y J, et al. Exosomal lncRNA GAS5 regulates the apoptosis of macrophages and vascular endothelial cells in atherosclerosis. PLoS One, 2017, 12(9):e0185406.
[19] Kern C, Wang Y, Chitwood J, et al. Genome-wide identification of tissue-specific long non-coding RNA in three farm animal species. BMC Genomics, 2018, 19(1): 684.
[20] Zhu J, Kong F Y, Xing L, et al. Prognostic and clinicopathological value of long noncoding RNA XIST in cance. Clin. Chim. Acta, 2018, 479:43-47.
[21] Dang Y, Lan F H, Ouyang X J, et al. Expression and clinical significance of long non-coding RNA HNF1A-AS1 in human gastric cancer. World J. Surg. Oncol., 2015, 13: 302.
[22] Lu D P, Luo P, Wang Q, et al. lncRNA PVT1 in cancer: A review and meta-analysis. Clin Chim Acta, 2017, 474:1-7.
[23] Han P, Li J W, Zhang B M, et al. The lncRNA CRNDE promotes colorectal cancer cell proliferation and chemoresistance via miR-181a-5p-mediated regulation of Wnt/β-catenin signaling. Mol. Cancer, 2017, 16(1):9.
[24] Ma T T, Zhou L Q, Xia J H, et al. LncRNA PCAT-1 regulates the proliferation, metastasis and invasion of cervical cancer cells. Eur. Rev. Med. Pharmacol. Sci., 2018, 22(7):1907-1913.
[25] Hartke J, Johnson M, Ghabril M. The diagnosis and treatment of hepatocellular carcinoma. Semin. Diagn. Pathol., 2017, 34(2):153-159.
[26] Ko K L, Mak L Y, Cheung K S, et al. Hepatocellular carcinoma: Recent advances and emerging medical therapies. F1000Res., 2020, 9:F1000 Faculty Rev-620.
[27] Craig A J, Felden J V, Lezana T G, et al. Tumour evolution in hepatocellular carcinoma. Nat. Rev. Gastroenterol. Hepatol., 2020, 17(3):139-152.
[28] Adams C M, Ebert S M, Dyle M C. Role of ATF4 in skeletal muscle atrophy. Curr. Opin. Clin. Nutr. Metab. Care, 2017, 20(3):164-168.
[29] Bader J E, Voss K, Rathmell J C. Targeting metabolism to improve the tumor microenvironment for cancer immunotherapy. Mol. Cell, 2020, 78(6):1019-1033.
[30] Li X X, Wang Z J, Zheng Y, et al. Nuclear receptor Nur77 facilitates melanoma cell survival under metabolic stress by protecting fatty acid oxidation. Mol. Cell, 2018, 69(3): 480-492. e7.
[31] Ye J B, Kumanova M, Hart L S, et al. The GCN2-ATF4 pathway is critical for tumour cell survival and proliferation in response to nutrient deprivation. EMBO J., 2010, 29(12):2082-2096.
[32] Dey S, Sayers C M, Verginadis I I, et al. ATF4-dependent induction of heme oxygenase 1 prevents anoikis and promotes metastasis. J. Clin. Invest., 2015, 125(7):2592-2608.
[33] Han J, Back S H, Hur J, et al. ER-stress-induced transcriptional regulation increases protein synthesis leading to cell death. Nat. Cell Biol., 2013, 15(5):481-490.
[34] Xiao Z D, Han L, Lee H, et al. Energy stress-induced lncRNA FILNC1 represses c-Myc-mediated energy metabolism and inhibits renal tumor development. Nat. Commun., 2017, 8(1):783.
[35] Liu X W, Xia Z D, Han L, et al. LncRNA NBR2 engages a metabolic checkpoint by regulating AMPK under energy stress. Nat. Cell Biol., 2016, 18(4):431-442.

长链非编码 RNA GIMA 通过抑制 ATF4 促进代谢压力下肝癌细胞的存活

王红,罗晶晶,王晨峰,张光,梅一德*, 杨洋*
中国科学技术大学生命科学与医学部基础医学学院,安徽合肥 230027
* 通讯作者. E-mail: meiyide@ustc.edu.cn; yangyang07@ustc.edu.cn

摘要: 肿瘤细胞通常处于营养匮乏的微环境中,细胞会产生一系列的适应性反应来维持代谢压力下的存活与增殖. 然而长链非编码 RNA(long non-coding RNA, lncRNA)在这一过程中的调控作用并不清楚. 为了探究 lncRNA 是否参与调控代谢压力下肝癌细胞的存活,转录组测序鉴定出一个受葡萄糖缺乏诱导的 lncRNA GIMA(glucose-deprivation induced modulator of ATF4),且 GIMA 的无糖上调依赖于 ATF4 的激活. 荧光素酶实验(luciferase assay)和染色质免疫共沉淀实验(chromatin immunoprecipitation assay,ChIP)表明 GIMA 是 ATF4 的转录靶基因. 进一步研究发现,GIMA 通过抑制 ATF4 的表达来促进葡萄糖缺乏条件下肝癌细胞的存活. 以上结果暗示了 GIMA 可能是一个新的肝癌治疗潜在靶点.

关键词: 长链非编码 RNA;GIMA;肝癌;葡萄糖缺乏;细胞存活